

**UNIVERSIDAD SAN FRANCISCO DE QUITO USFQ**

**Colegio de Ciencias e Ingeniería**

**Small-Signal Model of a Buck-Boost Four Port Converter**

**Martin Davide Crespo Ruiz**

**Ingeniería Electrónica y Automatización**

Trabajo de fin de carrera presentado como requisito  
para la obtención del título de

**INGENIERO EN ELECTRÓNICA**

Quito, 7 de agosto de 2023

# **UNIVERSIDAD SAN FRANCISCO DE QUITO USFQ**

**Colegio de Ciencias e Ingeniería**

## **HOJA DE CALIFICACIÓN DE TRABAJO DE FIN DE CARRERA**

**Small-Signal Model of a Buck-Boost Four Port Converter**

**Martin Davide Crespo Ruiz**

**Nombre del profesor, título académico: Alberto Sánchez, PhD**

Quito, 7 de agosto de 2023

## © DERECHOS DE AUTOR

Por medio del presente documento certifico que he leído todas las Políticas y Manuales de la Universidad San Francisco de Quito USFQ, incluyendo la Política de Propiedad Intelectual USFQ, y estoy de acuerdo con su contenido, por lo que los derechos de propiedad intelectual del presente trabajo quedan sujetos a lo dispuesto en esas Políticas.

Asimismo, autorizo a la USFQ para que realice la digitalización y publicación de este trabajo en el repositorio virtual, de conformidad a lo dispuesto en la Ley Orgánica de Educación Superior del Ecuador.

Nombres y apellidos: Martin Davide Crespo Ruiz

Código: 00208828

Cédula de identidad: 0924853039

Lugar y fecha: Quito, 7 de agosto de 2023

## **ACLARACIÓN PARA PUBLICACIÓN**

**Nota:** El presente trabajo, en su totalidad o cualquiera de sus partes, no debe ser considerado como una publicación, incluso a pesar de estar disponible sin restricciones a través de un repositorio institucional. Esta declaración se alinea con las prácticas y recomendaciones presentadas por el Committee on Publication Ethics COPE descritas por Barbour et al. (2017) Discussion document on best practice for issues around theses publishing, disponible en <http://bit.ly/COPETHeses>.

## **UNPUBLISHED DOCUMENT**

**Note:** The following capstone project is available through Universidad San Francisco de Quito USFQ institutional repository. Nonetheless, this project – in whole or in part – should not be considered a publication. This statement follows the recommendations presented by the Committee on Publication Ethics COPE described by Barbour et al. (2017) Discussion document on best practice for issues around theses publishing available on <http://bit.ly/COPETHeses>.

## RESUMEN

Este trabajo presenta el desarrollo de un modelo de pequeña señal de un convertidor DC-DC Buck-Boost de Cuatro Puertos (BB-FPC). El BB-FPC consta de dos convertidores Buck-Boost y un convertidor PWM con desplazamiento de fase que es capaz de operar como interfaz a fuentes de energía renovables para su distribución y almacenamiento. El convertidor tiene cuatro puertos: dos de entrada, uno para el sistema de almacenamiento y uno para la carga aislada. El flujo de potencia entre los puertos no-aislados puede ser bidireccional y son controlados por los tiempos de trabajo de cada ramal del convertidor, mientras que el flujo de potencia hacia la carga es controlado por el desfase entre los pulsos PWM. El documento ilustra el desarrollo paso a paso para la obtención del modelo de pequeña señal del BB-FPC el cual describe la interacción entre las variables de control de entrada y los voltajes y corrientes de cada puerto.

**Palabras clave:** Convertidor multipuerto, sistema de energía renovable, convertidor DC-DC, modelo de pequeña señal, control PWM por desplazamiento de fase.

## ABSTRACT

This work presents the development of a small-signal model of the Buck-Boost Four Port DC-DC Converter (BB-FPC). The BB-FPC is composed of two Buck-Boost converters and a Phase-Shifted PWM that is capable of interfacing two sources of renewable energy for both distribution and storage. The converter has four ports: two for inputs, one for a storage system and one for the isolated load. Power flow between non-isolated ports can be bidirectional and is controlled by the duty cycle in each leg of the converter, whereas the power flow to the load is controlled by the phase-shift between the PWM waveforms. This documents illustrate the step-by-step process for the small-signal model of the BB-FPC that describes the interaction between the control input variables and the voltages and currents in each port.

**Key words:** Multiport converter, renewable energy system, DC-DC converter, small-signal model, phase-shifted PWM.

**TABLE OF CONTENTS**

I. Introduction .....	10
II. BB-FPC Review .....	10
III. Methodology .....	11
A. Small-Signal Modelling .....	11
B. Converter Simulation and Model Verification.....	12
IV. Converter Modelling.....	12
A. Boost Converter with Battery System as Load .....	12
1. Simulation Results .....	13
B. Dual Boost Converter with Battery System as Load.....	13
1. Simulation Results .....	15
C. Buck-Boost Four Port Converter.....	15
1. Simulation Results .....	17
V. Conclusions.....	18
References.....	18

**Table Index**

Table I. Boost circuit parameters .....	13
Table II. Dual Boost circuit parameters .....	15
Table III. BB-FPC small-signal ac equations .....	18
Table IV. BB-FPC circuit parameters.....	18



## Figure Index

Figure 1. Buck-Boost Four Port Converter circuit.....	11
Figure 2. BB-FPC waveforms and switching states .....	11
Figure 3. Boost Converter.....	12
Figure 4. Boost Converter circuit and small-signal model comparison.....	13
Figure 5. Dual Boost Converter .....	14
Figure 6. Dual Boost Converter circuit and small-signal model comparison.....	15
Figure 7. BB-FPC .....	16
Figure 8. BB-FPC circuit and small-signal model comparison .....	17

# Small-Signal Model of a Buck-Boost Four Port Converter

Martin Davide Crespo Ruiz

Universidad San Francisco de Quito USFQ, Colegio de Ciencias e Ingenierías, Quito 170901, Ecuador

Email: mdcrespo@estud.usfq.edu.ec

## I. INTRODUCTION

In recent years, Multiport Converters (MPCs) have been a rising trend due to their utility when interfacing with renewable energy sources. These renewable energy sources are intermittent because they depend on climatic conditions of the zone [1], this cause the need to smooth the variations in power generation. To solve this, the use of a Energy Storage System (ESS) is employed. MPCs offers low cost, high power density, high efficiency, multi-channel PV panels and hybrid PV when interfacing power terminals [2], these characteristics make them ideal for interfacing renewable sources of energy.

MPCs are commonly classified as fully isolated, fully non-isolated and partly isolated. The topologies of MPCs are usually derived from other well known DC-DC converter topologies as Buck-Boost, SEPIK, CUK and others [3]. The problem with MPCs is the difficulty to control the system due to the use of multiple switches and the possibility of bidirectional power flow. To design a control system, a dynamic model is needed. This model tells us how variations in the inputs affects the outputs, to mathematically model a non-linear system, small-signal modelling is commonly used. This paper proposes a small-signal model of the Buck-Boost Four Port Converter (BB-FPC).

## II. BB-FPC REVIEW

The BB-FPC is a partly isolated MPC that is derived from both a Full Bridge Converter (FBC) and a Bidirectional DC-DC Converter (BDC) [2]. The schematic for the BB-FPC is shown in Fig. 1. The diagram shows that the converter has two PV ports, a Battery Energy Storage System (BESS) and one output port. It also consists of two switching legs, a transformer with its respective leakage inductance, a capacitor to avoid DC current into the transformer, a full bridge rectifier and a LC filter. Each switching leg consist of two power devices S1, S2 for Leg 1 and S3, S4 for Leg 2. Both switches from each leg must act in complementary state to avoid short circuit. These power devices control the modes of operation of the BB-FPC, this modes of operation depends on the climatic conditions of the environment and secures a constant voltage at the output.

The modes of operation are:

- Mode A: When both PV (Photovoltaic) panels are not capable of delivering energy, the battery is the only supplier.

- Mode B: When PV panels and BESS supply the load (controlled by a Maximum Power Point Tracking 'MPPT' algorithm).
- Mode C: When PV panels power is greater than demanded so they both supply the load and battery.

Each switching leg can act as a Buck when power is delivered from the BESS to the load, or as a Boost when PV panels deliver to the BESS and/or the load. Power delivered to the load is controlled as a Phase-Shifting Pulse Width Modulation (PS-PWM) Control Scheme. Because the BB-FPC acts similar to a PS-PWM converter, the BB-FPC is capable of achieving Zero Voltage Switching (ZVS), an analysis on the conditions to achieve ZVS and small signal analysis are reviewed on [4] and [2]. The BB-FPC key waveforms and switching states are shown in Fig. 2. Define  $T_s$  as the time for one complete cycle of the BB-FPC,  $D_1$  as the duty cycle of S2,  $D_2$  as the duty cycle of S4 and  $\phi$  as the phase between the turn on of S4 and S2. Additionally a time where the primary current transitions from positive to negative or negative to positive (see Fig. 2) is defined as  $dl$ , during these transitions the diodes from the full bridge rectifier have a freewheeling current through them. The converter six functioning states with its respective time duration are: (Refer Fig .2 for waveforms and Fig. 7 for circuit switching states)

- State I  $[(dl)Ts][t_0 - t_1]$ : While S3 is on and S4 off, at  $t_0$ , S2 is turned on and S1 is turned off. In this state exists an inductor current  $i_{L_o}$  freewheeling through the full bridge rectifier diodes. Because the diodes freewheels, the secondary winding of the transformer is shorted. Also inductor  $L_1$  is getting charged while  $L_2$  is being discharged.
- State II  $[(\phi)Ts][t_1 - t_2]$ : After the freewheeling of the diodes,  $D_{o1}$  and  $D_{o4}$  are reverse bias because  $v_{ab}$  is negative. The inductors remain in the same condition as State I.
- State III  $[(D_1 - \phi)Ts][t_2 - t_3]$ : While S2 is on and S1 off, at  $t_2$ , S4 is turned on and S3 is turned off. The inductor  $L_2$  starts charging while  $L_1$  remains charging. The voltage  $V_{ab}$  is equal to the voltage in the capacitor  $C_b$  and is close to zero.
- State IV  $[(dl)Ts][t_3 - t_4]$ : While S4 is on and S3 off, at  $t_3$ , S1 is turned on and S2 is turned off. Once again  $i_{L_o}$  freewheels through full bridge rectifier diodes  $D_{o1} - D_{o4}$  and the secondary of the transformer is shorted. Inductor

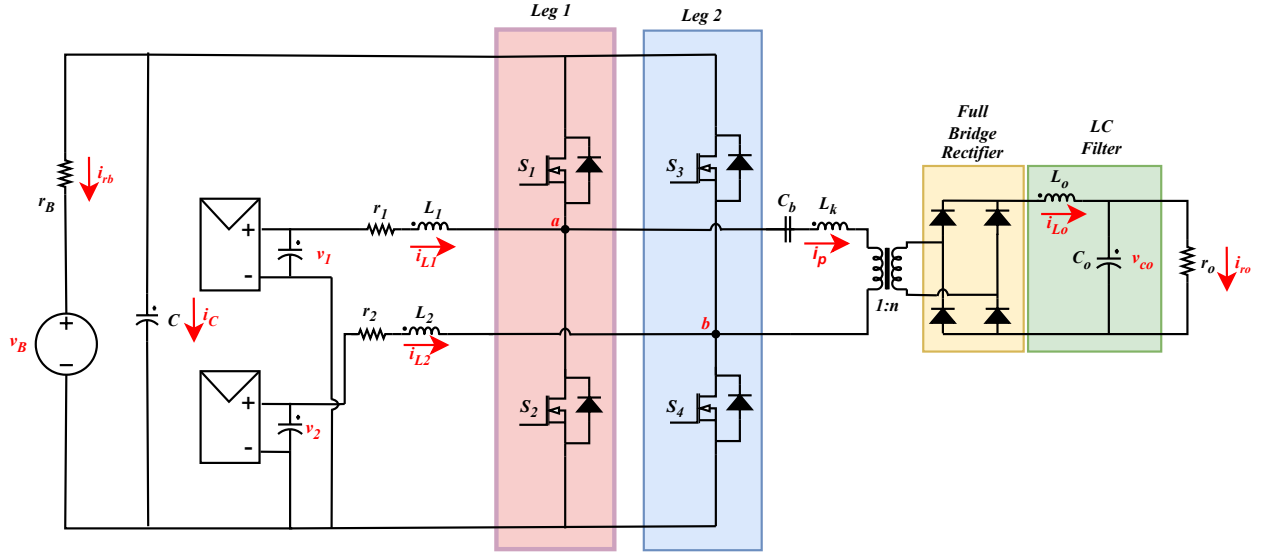


Fig. 1: Buck-Boost Four Port Converter circuit

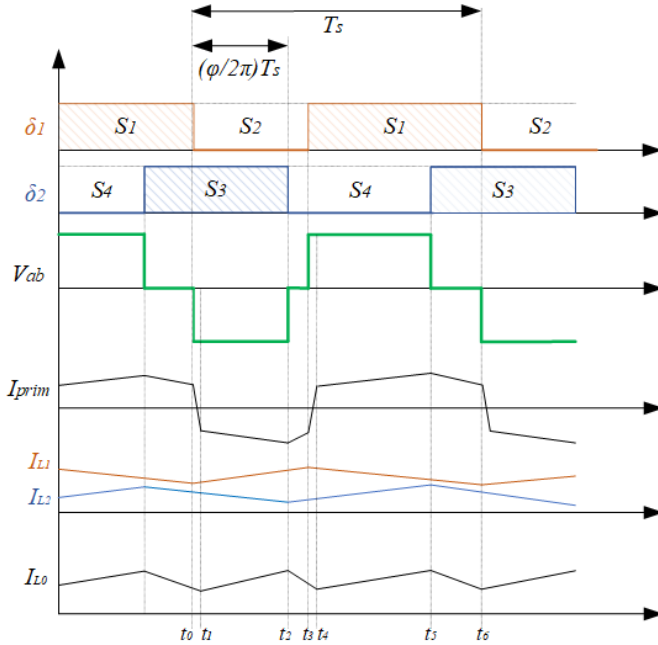


Fig. 2: BB-FPC waveforms and switching states [2].

$L_1$  starts to discharge while  $L_2$  continues charging.

- State V  $[(D_2 + \phi - D_1)T_s][t_4 - t_5]$ : After the freewheeling of the diodes,  $D_1$  and  $D_4$  are reverse bias because  $v_{ab}$  is positive. The inductors remain in the same condition as the State IV.
- State VI  $(1 - \phi - D_2)T_s][t_5 - t_6]$ : While S1 is on and S2 off, at  $t_5$ , S3 is turned on and S4 is turned off. The inductor  $L_2$  starts to discharge while  $L_1$  remains also discharging. The voltage  $V_{ab}$  is equal to the voltage in the capacitor  $C_b$  and is close to zero.

To control the BB-FPC we got the three control variables  $D_1$ ,  $D_2$  and  $\phi$ . From [2] it states that to be able to fully control the BB-FPC there are two constraints that we need

to follow:

$$\frac{\phi}{2\pi} \leq D_1 \quad (1)$$

$$\frac{\phi}{2\pi} \leq 1 - D_2 \quad (2)$$

When attempting to control the BB-FPC we must ensure these two conditions are simultaneously followed.

### III. METHODOLOGY

#### A. Small-Signal Modelling

To mathematically model the converter we employed a small-signal model, or properly called in this case, a linearized averaged small-signal model. The method for this type of modelling is deeply explained in [5]. Here is a brief explanation on the method. Firstly the small-signal ac model is obtained with the use of the small-ripple approximation, which is an approximation that ignores high frequency components of the signal. The low frequency components of the inductor and capacitor are expressed by the following equations:

$$\langle v_L(t) \rangle_{T_s} = L \left\langle \frac{di_L(t)}{dt} \right\rangle_{T_s} \quad (3)$$

$$\langle i_c(t) \rangle_{T_s} = C \left\langle \frac{dv_c(t)}{dt} \right\rangle_{T_s} \quad (4)$$

Where the “L” brackets refers to the averaging operator:

$$\langle x(t) \rangle_{T_s} = \frac{1}{T_s} \int_{t - \frac{T_s}{2}}^{t + \frac{T_s}{2}} x(\tau) d\tau \quad (5)$$

The small-ripple approximation is valid as long the quantities have small-ripple, are continuous in time and are not pulsating. So we apply this approximation to every capacitor and inductor of the converter for each switching state. Then we average the previous obtained equations over one period of the converter to obtain the averaged small-signal ac equations of the system. As a last step we linearize the model by expressing the

variables as a constant dc value plus a small ac value that varies in time. When linearizing the system we ensure the model is approximately linear to small changes in the input. By rearranging the terms on the linearized averaged small-signal model we obtain two set of equations, the ac equations that describe the dynamic of the system and the dc equations that describe the operating point of the system. This small signal model is capable of predicting the output when an small perturbation is introduced in the input, if the perturbation is too large the predicted output may be inaccurate due to the change of the operating point in the system.

### B. Converter Simulation and Model Verification

To verify that the small-signal model is working, the converter is implemented in the blockset version of Plexim's PLECS® where a perturbation is introduced in the input and then compared with the small-signal model that is implemented as a C S-function in Mathworks SIMULINK® that suffers the same perturbation.

## IV. CONVERTER MODELLING

Because the BB-FPC is a complex converter, this section models simpler converters and builds up to eventually the BB-FPC small-signal model.

### A. Boost Converter with a Battery System as Load

This converter is depicted in Fig. 3a, this is a boost converter in which  $V_1$  supplies the battery system. The battery system is represented as a constant voltage source [2], a resistance and a capacitor. The resistance  $R_b$  models the internal resistance of the battery, the capacitor  $C$  models the current from the battery as well as representing the decoupling capacitor of the battery and the diode  $D_1$  ensures  $V_1$  only delivers power. Defining  $T_s$  as the period of one cycle of the converter,  $D_1$  as the duty cycle of  $S_1$  and  $D_p$  as its complementary, the converter has two functioning states with a duration of  $(D_1)T_s$  in the first state and  $(D_p)T_s$  in the second one. The converter is analyzed by using the small-ripple approximation for the inductor and capacitor in each switching state:

State I  $[(D)T_s]$ [Refer to Fig. 3b]: In this state  $L_1$  is getting charged, the current through  $C$  and the voltage through  $L_1$  are represented by the following equations:

$$v_{L_1}(t) = L_1 \frac{di_{L_1}(t)}{dt} = v_1(t) \quad (6)$$

$$i_c(t) = C \frac{dv_c(t)}{dt} = \frac{V_b - v_c(t)}{R_b} \quad (7)$$

State II  $[(D_p)T_s]$ [Refer to Fig.3c]: Now  $L_1$  is getting discharged, the equations of this state are:

$$v_{L_1}(t) = L_1 \frac{di_{L_1}(t)}{dt} = v_1(t) - v_c(t) \quad (8)$$

$$i_c(t) = C \frac{dv_c(t)}{dt} = \frac{V_b - v_c(t)}{R_b} + i_{L_1}(t) \quad (9)$$

Because we are interested in the response of the model to a change in the control variable  $D_1$  and its complementary  $D_p$ , we express them as the time changing variables  $d_1(t)$

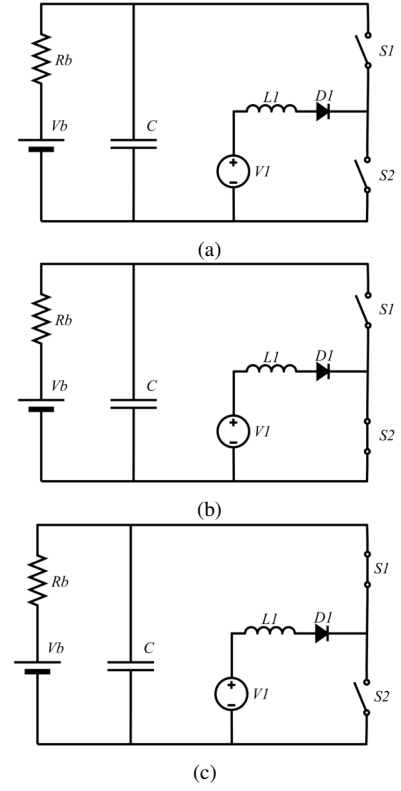


Fig. 3: Boost Converter: (a) Equivalent circuit (b) State I (c) State II

and  $d_p(t)$  respectively. The averaged equations are obtained by averaging the equations (6) and (7) with (8) and (9) respectively. This results in:

$$\langle v_{L_1}(t) \rangle_{T_s} = L_1 \langle \frac{di_{L_1}(t)}{dt} \rangle_{T_s} = v_1(t) - v_c(t)d_p(t) \quad (10)$$

$$\langle i_c(t) \rangle_{T_s} = C \langle \frac{dv_c(t)}{dt} \rangle_{T_s} = \frac{V_b - v_c(t)}{R_b} + i_{L_1}(t)d_p(t) \quad (11)$$

Equations (10) and (11) are a set of non-linear differential equations, so, with the purpose of linearizing the system, we express the inputs and its responses as a dc value plus a small ac variation assuming all transients have decayed.

$$\langle v_c(t) \rangle_{T_s} = V_c + \hat{v}_c(t)$$

$$\langle i_{L_1}(t) \rangle_{T_s} = I_{L_1} + \hat{i}_{L_1}(t)$$

$$\langle d_1(t) \rangle_{T_s} = D_1 + \hat{d}_1(t)$$

$$\langle d_p(t) \rangle_{T_s} = D_p - \hat{d}_1(t)$$

$$\langle v_1(t) \rangle_{T_s} = V_1 + \hat{v}_1(t)$$

The linearized averaged small-signal differential equations are:

$$L_1 \langle \frac{d(I_{L_1} + \hat{i}_{L_1}(t))}{dt} \rangle_{T_s} = V_1 - (V_c D_p - V_c \hat{d}_1(t) + \hat{v}_c(t) D_p - \hat{v}_c(t) \hat{d}_1(t)) \quad (12)$$

$$C \langle \frac{d(V_c + \hat{v}_c(t))}{dt} \rangle_{T_s} = \frac{V_b - V_c - \hat{v}_c(t)}{R_b} + I_{L_1} D_p - I_{L_1} \hat{d}_1(t) + D_p \hat{i}_{L_1}(t) - \hat{i}_{L_1}(t) \hat{d}_1(t) \quad (13)$$

Both the inductor voltage and the capacitor current values are zero in steady state, so, by collecting the DC terms of (12) and (13) we obtain the equations of their respective quiescent values:

$$0 = V_1 - V_c D_p \quad (14)$$

$$0 = \frac{V_b - V_c}{R_b} + I_{L_1} D_p \quad (15)$$

Because the multiplication of two small ac terms will lead to even a smaller ac term, the second order terms will be omitted for the models. The small-signal ac equations are:

$$L_1 \left\langle \frac{\hat{i}_{L_1}(t)}{dt} \right\rangle_{T_s} = \hat{v}_1(t) + V_c \hat{d}_1(t) - \hat{v}_c(t) D_p \quad (16)$$

$$C \left\langle \frac{d\hat{v}_c(t)}{dt} \right\rangle_{T_s} = \frac{-\hat{v}_c(t)}{R_b} - I_{L_1} \hat{d}_1(t) + D_p \hat{i}_{L_1}(t) \quad (17)$$

1) *Simulation Results:* The converter is working at 100KHz with the parameters listed in Table I. The system inputs are both  $D_1$  and  $V_1$  while the outputs are  $i_{L_1}$  and  $V_c$ . The perturbations introduced in the converter are square pulses with magnitude of 10% its input value as shown in Fig. 4a. The comparison between the converter response and small-signal model response to the perturbations introduced is shown in Fig. 4b, we can appreciate how the model response is almost identical to the converter response.

TABLE I: Boost Circuit Parameters

Component	Value
L1	72 [ $\mu$ H]
C	5 [mF]
$R_b$	0.1 [ $\Omega$ ]
$D_1$	0.6
$V_b$	72 [V]
$V_1$	50 [V]

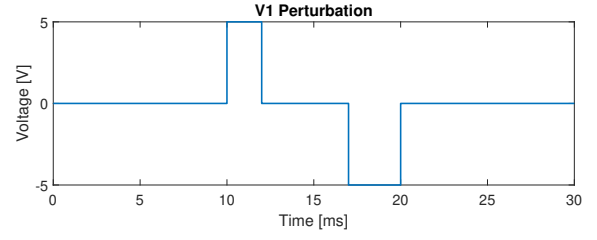
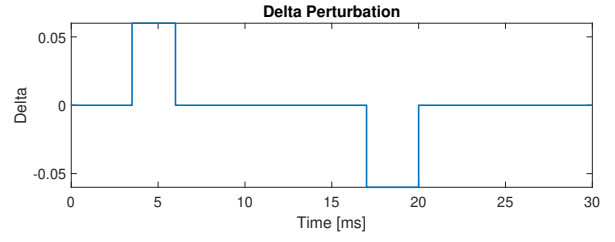
### B. Dual Boost Converter with a Battery System as Load

By attaching another boost converter in parallel to the previous converter we obtain a two input dual boost converter with a battery system as load which is depicted in Fig. 5. With this modification, we have two voltage sources that supply the battery. It was also necessary to introduce the resistors  $R_{l_1}$  and  $R_{l_2}$  to be able to model the inductor currents. Defining  $D_1$  as the duty cycle of S2,  $D_2$  as the duty cycle of S4 and  $\frac{\phi}{2\pi}$  as the phase between the turn on of S4 and S2. The converter is examined by its four switching states: State I [ $(\frac{\phi}{2\pi})T_s$ ][Refer to Fig. 5b]: At State I, S2 is turned on, S1 is turned off and S3 stays on. Inductor L1 is getting charged and L2 discharges. The equations of the current state are:

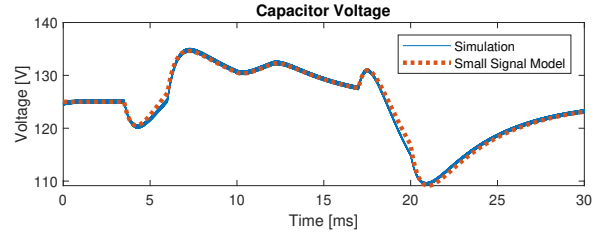
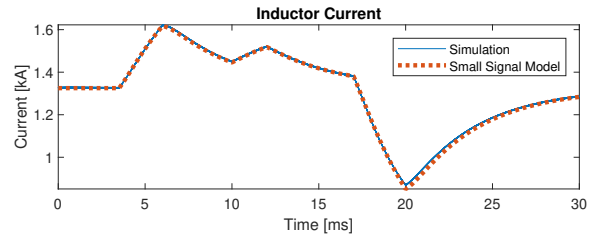
$$v_{L_1}(t) = \frac{di_{L_1}(t)}{dt} = v_1(t) - i_{L_1}(t)R_{l_1} \quad (18)$$

$$v_{L_2}(t) = \frac{di_{L_2}(t)}{dt} = v_2(t) - v_c(t) - i_{L_2}(t)R_{l_2} \quad (19)$$

$$i_c(t) = \frac{dv_c(t)}{dt} = \frac{V_b - v_c(t)}{R_b} + i_{L_2}(t) \quad (20)$$



(a)



(b)

Fig. 4: Boost Converter circuit and small-signal model response comparison: (a) Input perturbations (b) Output waveforms

State II [ $(D_1 - \frac{\phi}{2\pi})T_s$ ][Refer to Fig. 5c]: At State II, S4 is turned on, S3 is turned off and S2 stays on. Both L1 and L2 are getting charged. The equations of State II are:

$$v_{L_1}(t) = \frac{di_{L_1}(t)}{dt} = v_1(t) - i_{L_1}(t)R_{l_1} \quad (21)$$

$$v_{L_2}(t) = \frac{di_{L_2}(t)}{dt} = v_2(t) - i_{L_2}(t)R_{l_2} \quad (22)$$

$$i_c(t) = \frac{dv_c(t)}{dt} = \frac{V_b - v_c(t)}{R_b} \quad (23)$$

State III [ $(D_2 + \frac{\phi}{2\pi} - D_1)T_s$ ][Refer to Fig. 5d]: At State III, S1 is turned on, S2 is turned off and S4 stays on. While L1 discharges, L2 is getting charged. The equations of State III

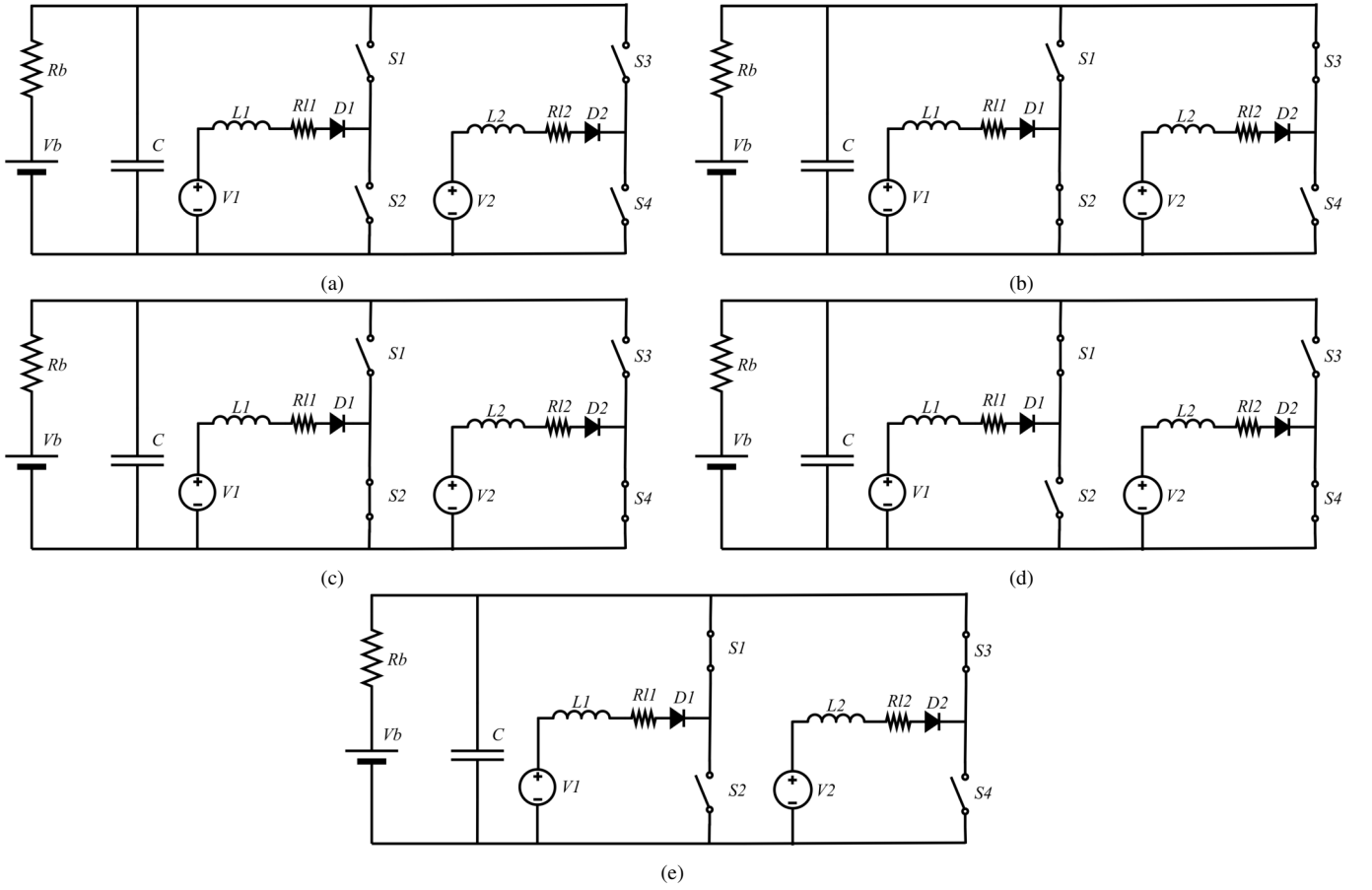


Fig. 5: Dual Boost Converter: (a) Equivalent circuit (b) State I (c) State II (d) State III (e) State IV

become:

$$v_{L_1}(t) = \frac{di_{L_1}(t)}{dt} = v_1(t) - v_c(t) - i_{L_1}(t)R_{l_1} \quad (24)$$

$$v_{L_2}(t) = \frac{di_{L_2}(t)}{dt} = v_2(t) - i_{L_2}(t)R_{l_2} \quad (25)$$

$$i_c(t) = \frac{dv_c(t)}{dt} = \frac{V_b - v_c(t)}{R_b} + i_{L_1}(t) \quad (26)$$

State IV  $[(1-D_2-\frac{\phi}{2\pi})T_s]$ [Refer to Fig. 5e]: At State IV, \$S\_3\$ is turned on, \$S\_4\$ is turned off and \$S\_1\$ stays on. Both \$L\_1\$ and \$L\_2\$ are getting discharged. The equations of State IV become:

$$v_{L_1}(t) = \frac{di_{L_1}(t)}{dt} = v_1(t) - v_c(t) - i_{L_1}(t)R_{l_1} \quad (27)$$

$$v_{L_2}(t) = \frac{di_{L_2}(t)}{dt} = v_2(t) - v_c(t) - i_{L_2}(t)R_{l_2} \quad (28)$$

$$i_c(t) = \frac{dv_c(t)}{dt} = \frac{V_b - v_c(t)}{R_b} + i_{L_1}(t) + i_{L_2}(t) \quad (29)$$

As in the single boost converter, we are interested in the response of the model to changes in the control variables, in this case, \$D\_1\$, \$D\_2\$ and \$\frac{\phi}{2\pi}\$. Expressing them as time changing variables \$d\_1(t)\$, \$d\_2(t)\$ and \$\frac{\phi(t)}{2\pi}\$ respectively. The small-ripple

approximated averaged equations over one period are:

$$\langle v_{L_1}(t) \rangle_{T_s} = \langle \frac{di_{L_1}(t)}{dt} \rangle_{T_s} = v_1(t) + v_c(t)(d_1(t) - 1) - i_{L_1}(t)R_{l_1} \quad (30)$$

$$\langle v_{L_2}(t) \rangle_{T_s} = \langle \frac{di_{L_2}(t)}{dt} \rangle_{T_s} = v_2(t) + v_c(t)(d_2(t) - 1) - i_{L_2}(t)R_{l_2} \quad (31)$$

$$\langle i_c(t) \rangle_{T_s} = \langle \frac{dv_c(t)}{dt} \rangle_{T_s} = \frac{V_b - v_c(t)}{R_b} + i_{L_1}(t)(1 - d_1(t)) + i_{L_2}(t)(1 - d_2(t)) \quad (32)$$

To linearize the previous equations we express inputs and outputs as a dc value plus ac variations:

$$\begin{aligned} \langle V_c(t) \rangle_{T_s} &= V_c + \hat{v}_c(t) \\ \langle I_{L_1}(t) \rangle_{T_s} &= I_{L_1} + \hat{i}_{L_1}(t) \\ \langle I_{L_2}(t) \rangle_{T_s} &= I_{L_2} + \hat{i}_{L_2}(t) \\ \langle D_1(t) \rangle_{T_s} &= D_1 + \hat{d}_1(t) \\ \langle D_2(t) \rangle_{T_s} &= D_2 + \hat{d}_2(t) \end{aligned}$$

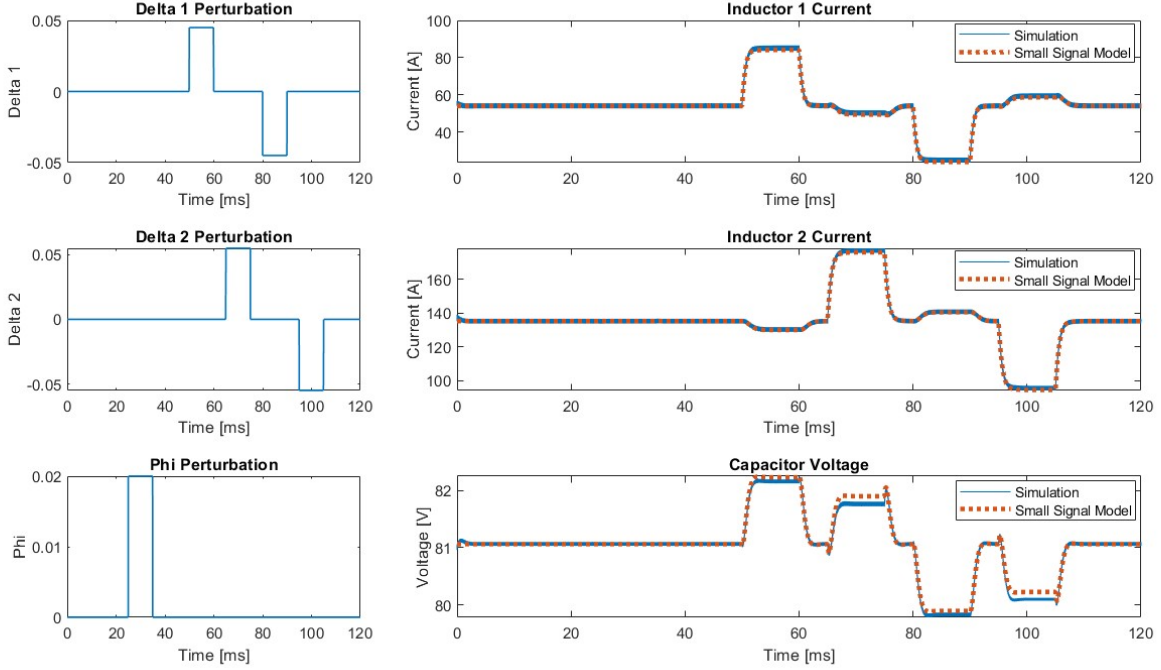


Fig. 6: Dual Boost Converter circuit and small-signal model response comparison

By expanding the small-ripple approximated averaged equations and knowing both the inductor voltage and the capacitor current values are zero in steady state, the dc equations of the converter are:

$$0 = V_1 + V_c(D_1 - 1) - I_{L_1}R_{l_1} \quad (33)$$

$$0 = V_2 + V_c(D_2 - 1) - I_{L_2}R_{l_2} \quad (34)$$

$$0 = \frac{V_b - V_c}{R_b} + I_{L_1}(1 - D_1) + I_{L_2}(1 - D_2) \quad (35)$$

And the first order small ac equations of the Dual Boost Converter with Battery System as Load are:

$$L_1 \left\langle \frac{\hat{i}_{L_1}(t)}{dt} \right\rangle_{T_s} = \hat{v}_1 + V_c \hat{d}_1(t) + \hat{v}_c(t)(D_1 - 1) \quad (36)$$

$$L_2 \left\langle \frac{\hat{i}_{L_2}(t)}{dt} \right\rangle_{T_s} = \hat{v}_2 + V_c \hat{d}_2(t) + \hat{v}_c(t)(D_2 - 1) \quad (37)$$

$$C_b \left\langle \frac{d\hat{v}_c(t)}{dt} \right\rangle_{T_s} = \frac{-\hat{v}_c(t)}{R_b} - I_{L_1} \hat{d}_1(t) + \hat{i}_{L_1}(1 - D_1) - I_{L_2} \hat{d}_2(t) + \hat{i}_{L_2}(1 - D_2) \quad (38)$$

1) *Simulation Results:* The converter is working at 100KHz with the parameters listed in Table II. The system inputs are  $D_1$ ,  $D_2$ ,  $\frac{\phi}{2\pi}$ ,  $V_1$  and  $V_2$  while the outputs are  $i_{L_1}$ ,  $i_{L_2}$  and  $V_c$ . The perturbations introduced in the converter are square pulses in the control variables  $D_1$ ,  $D_2$  and  $\frac{\phi}{2\pi}$  with magnitude of 10% of its input value as shown in the left column of Fig. 6. The comparison between the converter response and small-signal model response to the perturbations introduced in the right column of is shown in Fig.6, we can appreciate how the

TABLE II: Dual Boost Circuit Parameters

Component	Value
$V_b$	72 [V]
$V_1 \& V_2$	50 [V]
$L_1 \& L_2$	72 [ $\mu$ H]
$C$	5 [mF]
$R_b \& R_{l_1} \& R_{l_2}$	0.1 [ $\Omega$ ]
$D_1$	0.45
$D_2$	0.55
$\frac{\phi}{2\pi}$	0.2
n	1

model response is almost identical to the converter response. It can also be seen that the control variable  $D_1$  is highly coupled to the inductor current  $i_{L_1}$  and the capacitor voltage  $V_c$  and almost decoupled from the inductor current  $i_{L_1}$ . The control variable  $D_2$  has a similar behavior, affecting mainly to  $i_{L_2}$  and  $V_c$  while almost no effect on  $i_{L_1}$ . Interestingly a  $\frac{\phi}{2\pi}$  perturbation has no effect on the output variables.

### C. Buck-Boost Four Port Converter

The BB-FPC is finally build by attaching the transformer, the LC filter, the load and by adding the two important design elements that are the block capacitor  $C_b$  and the leakage inductance of the transformer  $L_k$ . The capacitor  $C_b$  is used to avoid DC current entering the transformer. While the inductance  $L_k$  is an important design value when trying to achieve Zero Voltage Switching (ZVS) [2]. Even though the capacitor  $C_b$  and the inductance  $L_k$  are fundamental for the converter design, it will be omitted in the small-signal model. This due to the signals going through these elements

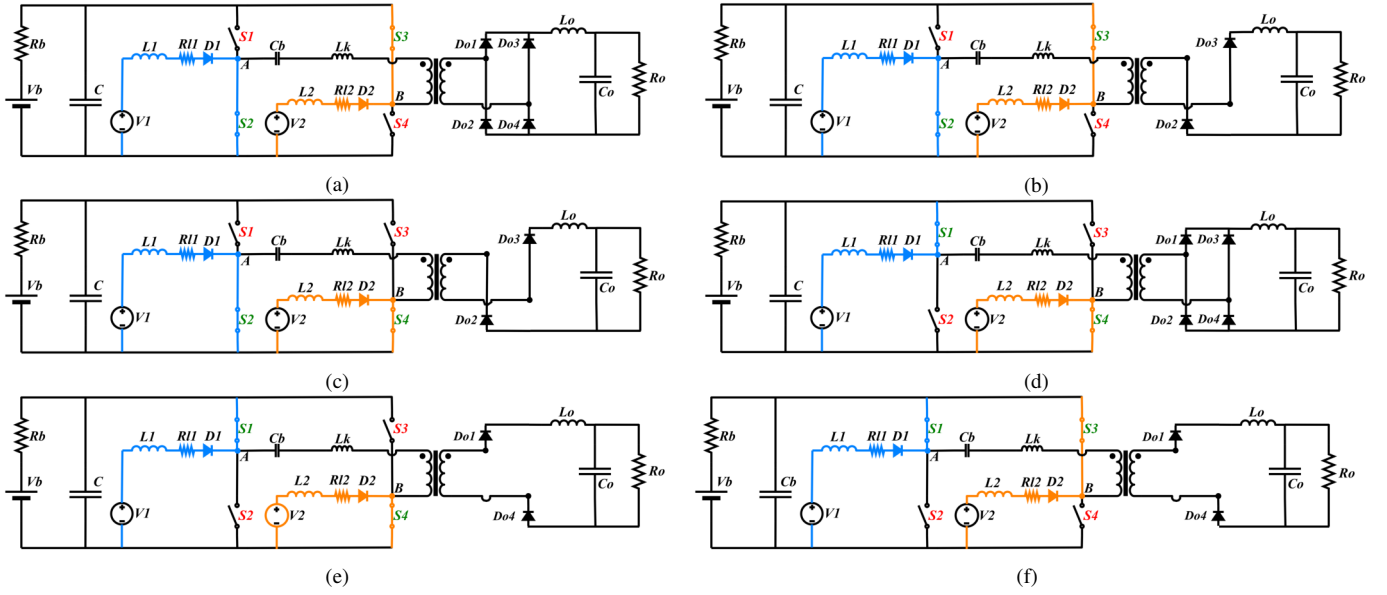


Fig. 7: BB-FPC: (a) Freewheeling diodes State (b) State I (c) State II (d) Freewheeling diodes State (e) State III (f) State IV

or through nodes A and B (Fig. 1) are large signals with sudden large changes which will not be suited for a small-signal model, for this reason, the dynamic behavior of the capacitor  $C_b$  and inductance  $L_k$  are omitted in the small signal model. Furthermore, the states where the current from the primary of the transformer transition from positive to negative and negative to positive are omitted. These are the states I and IV in which the diodes  $D_{o1} - D_{o4}$  have a freewheeling current. This simplification is possible if the inductance  $L_k$  is considerably smaller than the output inductance  $L_o$ , this ensures the transition of the primary current to be very fast.

$$n^2 L_k \ll L_o \quad (39)$$

With this approximation the switching states I and IV are absorbed in states II and V respectively. Now we make the small signal model of the BB-FPC by modeling the dynamic behavior from  $L_1, L_2, C_b, L_o$  and  $C_o$  in the following four different switching states:

State I  $[(\frac{\phi}{2\pi})T_s]$ [Refer to Fig. 7b]: At State I, S2 is turned on, S1 is turned off and S3 stays on. Inductor  $L_1$  is getting charged and  $L_2$  discharges. The equations of the current state are:

$$v_{L_1}(t) = L_1 \frac{di_{L_1}(t)}{dt} = v_1(t) - i_{L_1}(t)R_{l_1} \quad (40)$$

$$v_{L_2}(t) = L_2 \frac{di_{L_2}(t)}{dt} = v_2(t) - v_c(t) - i_{L_2}(t)R_{l_2} \quad (41)$$

$$i_c(t) = C \frac{dv_c(t)}{dt} = \frac{V_b - v_c(t)}{r_b} + i_{L_2}(t) - ni_{L_o}(t) \quad (42)$$

$$v_{L_o}(t) = L_o \frac{di_{L_o}(t)}{dt} = n(v_c(t) + v_{c_b}(t)) - v_{c_o}(t) \quad (43)$$

$$i_{c_o}(t) = C_o \frac{dv_{c_o}(t)}{dt} = i_{L_o}(t) - \frac{v_{c_o}(t)}{R_o} \quad (44)$$

State II  $[(D_1 - \frac{\phi}{2\pi})T_s]$ [Refer to Fig. 5c]: At State II, S4 is turned on, S3 is turned off and S2 stays on. Both  $L_1$  and  $L_2$  are getting charged. The equations of State II are:

$$v_{L_1}(t) = L_1 \frac{di_{L_1}(t)}{dt} = v_1(t) - i_{L_1}(t)R_{l_1} \quad (45)$$

$$v_{L_2}(t) = L_2 \frac{di_{L_2}(t)}{dt} = v_2(t) - i_{L_2}(t)R_{l_2} \quad (46)$$

$$i_c(t) = C \frac{dv_c(t)}{dt} = \frac{V_b - v_c(t)}{r_b} \quad (47)$$

$$v_{L_o}(t) = L_o \frac{di_{L_o}(t)}{dt} = nv_{c_b}(t) - v_{c_o}(t) \quad (48)$$

$$i_{c_o}(t) = C_o \frac{dv_{c_o}(t)}{dt} = i_{L_o}(t) - \frac{v_{c_o}(t)}{R_o} \quad (49)$$

State III  $[(D_2 + \frac{\phi}{2\pi} - D_1)T_s]$ [Refer to Fig. 5d]: At State III, S1 is turned on, S2 is turned off and S4 stays on. While  $L_1$  discharges,  $L_2$  is getting charged. The equations of State III become:

$$v_{L_1}(t) = L_1 \frac{di_{L_1}(t)}{dt} = v_1(t) - i_{L_1}(t)R_{l_1} - v_c(t) \quad (50)$$

$$v_{L_2}(t) = L_2 \frac{di_{L_2}(t)}{dt} = v_2(t) - i_{L_2}(t)R_{l_2} \quad (51)$$

$$i_c(t) = C \frac{dv_c(t)}{dt} = \frac{V_b - v_c(t)}{r_b} + i_{L_1}(t) - ni_{L_o}(t) \quad (52)$$

$$v_{L_o}(t) = L_o \frac{di_{L_o}(t)}{dt} = n(v_c(t) + v_{c_b}(t)) - v_{c_o}(t) \quad (53)$$

$$i_{c_o}(t) = C_o \frac{dv_{c_o}(t)}{dt} = i_{L_o}(t) - \frac{v_{c_o}(t)}{R_o} \quad (54)$$

State IV  $[(1 - D_2 - \frac{\phi}{2\pi})T_s]$ [Refer to Fig. 5e]: At State IV, S3 is turned on, S4 is turned off and S1 stays on. Both  $L_1$  and  $L_2$  are getting discharged. The equations of State IV become:



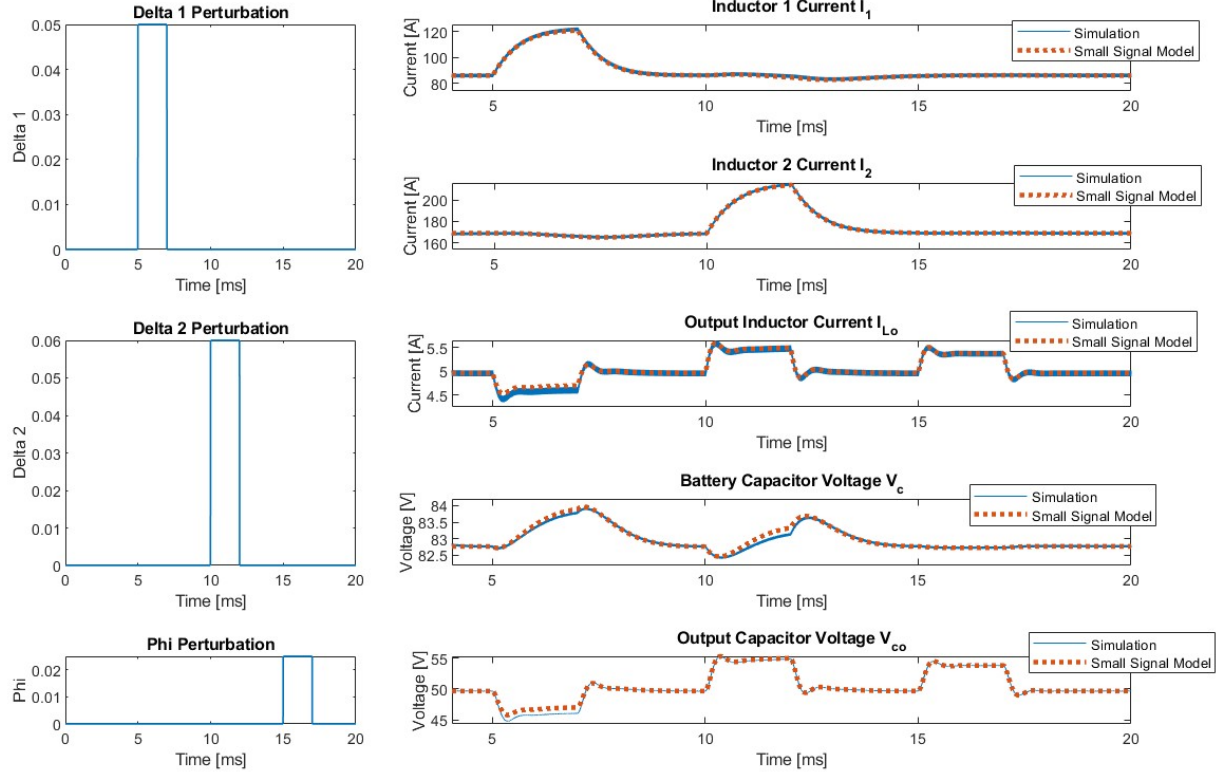


Fig. 8: BB-FPC circuit and small-signal model response comparison

$$v_{L_1}(t) = L_1 \frac{di_{L_1}(t)}{dt} = v_1(t) - i_{L_1}(t)R_{l_1} - v_c(t) \quad (55)$$

$$v_{L_2}(t) = L_2 \frac{di_{L_2}(t)}{dt} = v_2(t) - i_{L_2}(t)R_{l_2} - v_c(t) \quad (56)$$

$$i_c(t) = C \frac{dv_c(t)}{dt} = \frac{V_b - v_c(t)}{r_b} + i_{L_1}(t) + i_{L_2}(t) \quad (57)$$

$$v_{L_o}(t) = L_o \frac{di_{L_o}(t)}{dt} = -nv_{c_b}(t) - v_{c_o}(t) \quad (58)$$

$$i_{c_o}(t) = C_o \frac{dv_{c_o}(t)}{dt} = i_{L_o}(t) - \frac{v_{c_o}(t)}{R_o} \quad (59)$$

By averaging the previous equations over one converter cycle and linearizing the variables  $i_{L_1}$ ,  $i_{L_2}$ ,  $v_c$ ,  $v_{c_o}$ ,  $i_{L_o}$ ,  $D_1$ ,  $D_2$ , and  $\frac{\phi}{2\pi}$  we get the first order small-signal ac equations listed in Table III, and the dc equations of the BB-FPC listed below:

$$0 = \frac{V_b - V_c}{r_b} + I_{L_1}(1 - D_1) + I_{L_2}(1 - D_2) + n(D_1 - D_2 - 2\frac{\phi}{2\pi})I_{L_o} \quad (60)$$

$$0 = I_{L_o} - \frac{V_{c_o}}{R_o} \quad (61)$$

$$0 = V_1 + V_C(D_1 - 1) - I_{L_1}R_1 \quad (62)$$

$$0 = V_2 + V_C(D_2 - 1) - I_{L_2}R_2 \quad (63)$$

$$0 = n(D_2 - D_1 + 2\frac{\phi}{2\pi})V_c - V_{c_o} + n(2D_1 - 1)V_{c_b} \quad (64)$$

Even though we omitted the dynamic of the capacitor  $C_b$ , the steady state voltage through it is not zero due to asymmetrical operation on the switching legs, in [2] is shown the voltage  $V_{c_b}$  is the one displayed below:

$$0 = V_c(D_2 - D_1) - V_{c_b} \quad (65)$$

1) *Simulation Results:* The converter is working at 100KHz with the parameters listed in Table IV. The system inputs are  $D_1$ ,  $D_2$ ,  $\frac{\phi}{2\pi}$ ,  $V_1$  and  $V_2$  while the outputs are  $i_{L_1}$ ,  $i_{L_2}$ ,  $i_{L_o}$ ,  $V_c$  and  $V_{c_o}$ . The perturbations introduced in the converter are square pulses in the control variables  $D_1$ ,  $D_2$  and  $\frac{\phi}{2\pi}$  with magnitude of 10% of its input value as shown in the left column of Fig. 8. The comparison between the converter response and small-signal model response to the perturbations introduced in the right column of Fig. 8, we can recognize how the model response is almost identical to the converter response. In the output variables  $i_{L_o}$  and  $V_{c_o}$  exists a small bias error probably caused due to the omitted dynamics of  $C_b$  and  $L_k$ . It can also be seen that the control variable  $D_1$  is highly coupled to the output variables  $i_{L_1}$ ,  $i_{L_o}$ ,  $V_c$  and  $V_{c_o}$  while almost decoupled from the inductor current  $i_{L_2}$ . The control variable  $D_2$  has a similar behavior, affecting mainly to  $i_{L_2}$ ,  $i_{L_o}$ ,  $V_c$  and  $V_{c_o}$  while almost no effect on  $i_{L_1}$ . Finally, a  $\frac{\phi}{2\pi}$  perturbation is highly coupled to variables  $V_{c_o}$  and  $i_{L_o}$  and almost decoupled to variables  $i_{L_1}$ ,  $i_{L_2}$  and  $V_c$ . To be able

TABLE III: BB-FPC Small-signal ac equations

$$\begin{aligned}
L_1 \left\langle \frac{\hat{i}_{L_1}(t)}{dt} \right\rangle_{Ts} &= \hat{v}_1(t) + V_c \hat{d}_1(t) - (1 - D_1) \hat{v}_c(t) - R_{l_1} \hat{i}_{L_1}(t) \\
L_2 \left\langle \frac{\hat{i}_{L_2}(t)}{dt} \right\rangle_{Ts} &= \hat{v}_2(t) + V_c \hat{d}_2(t) - (1 - D_2) \hat{v}_c(t) - R_{l_2} \hat{i}_{L_2}(t) \\
C \left\langle \frac{d\hat{v}_c(t)}{dt} \right\rangle_{Ts} &= \frac{-\hat{v}_c(t)}{R_b} + (1 - D_1) \hat{i}_{L_1}(t) + (1 - D_2) \hat{i}_{L_2}(t) + n(D_1 - D_2 + 2\frac{\phi}{2\pi}) \hat{i}_{L_o}(t) + (nI_{L_o} - I_{L_1}) \hat{d}_1(t) - (nI_{L_o} + I_{L_2}) \hat{d}_2(t) - 2nI_{L_o} \frac{\hat{\phi}}{2\pi} \\
L_o \left\langle \frac{d\hat{i}_{L_o}(t)}{dt} \right\rangle_{Ts} &= n(D_2 - D_1 + 2\frac{\phi}{2\pi}) \hat{v}_c(t) + n(2D_1 - 1) \hat{v}_c(t) + n(2V_{c_b} - V_c) \hat{d}_1(t) + nV_c \hat{d}_2(t) + 2nV_c \frac{\hat{\phi}}{2\pi} \\
C_o \left\langle \frac{d\hat{v}_{c_o}(t)}{dt} \right\rangle_{Ts} &= -\frac{\hat{v}_{c_o}(t)}{R_o} + \hat{i}_{L_o}(t)
\end{aligned}$$

to certainly know the limitations of the small-signal model, an in depth small-signal analysis is required.

TABLE IV: BB-FPC Circuit Parameters

Component	Value
$V_b$	72 [V]
$V_1 \& V_2$	50 [V]
$L_1 \& L_2$	72 [ $\mu$ H]
$L_k$	0.1 [ $\mu$ H]
$L_o$	1 [mH]
$C$	5 [mF]
$C_b$	15 [ $\mu$ F]
$C_o$	10 [ $\mu$ F]
$R_b \& R_{l_1} \& R_{l_2}$	0.1 [ $\Omega$ ]
$R_o$	10 [ $\Omega$ ]
$D_1$	0.5
$D_2$	0.6
$\frac{\phi}{2\pi}$	0.25
$n$	1

## V. CONCLUSIONS

In this paper, a small-signal model for the BB-FPC has been proposed using small-ripple approximation, averaging

and linearization. The linear system obtained seems to correctly model both the dynamics and the steady state of the converter when a perturbation is introduced in the control input variables, small-signal analysis is required to designate the limits of the model. Furthermore the system indicates the different control inputs are highly coupled to different variables in the system, for a precise control of the BB-FPC, multi-variable control may be required.

## REFERENCES

- [1] IEA, "Renewables global energy review 2021 analysis," Apr 2021. [Online]. Available: <https://www.iea.org/reports/global-energy-review-2021/renewables>
- [2] H. Wu, P. Xu, H. Hu, Z. Zhou, and Y. Xing, "Multiport converters based on integration of full-bridge and bidirectional dc-dc topologies for renewable generation systems," *IEEE transactions on industrial electronics*, vol. 61, no. 2, pp. 856–869, 2013.
- [3] D. Valencia, N. Pozo, and A. Sánchez, "Multi-variable fuzzy+ pid control of a buck-boost four port converter for renewable energy system," in *2022 IEEE International Autumn Meeting on Power, Electronics and Computing (ROPEC)*, vol. 6. IEEE, 2022, pp. 1–6.
- [4] V. Vlatkovic, J. A. Sabate, R. B. Ridley, F. C. Lee, and B. H. Cho, "Small-signal analysis of the phase-shifted pwm converter," *IEEE Transactions on power Electronics*, vol. 7, no. 1, pp. 128–135, 1992.
- [5] R. W. Erickson and D. Maksimovic, *Fundamentals of power electronics*. Springer Science & Business Media, 2007.